To cite this version :

Performance assessment of a standard radial turbine as turbo expander for an adapted solar concentration ORC

Michael Deligant[a,*], Quentin Danel[a], Farid Bakir[a]

a DynFluid Lab - EA92, Arts et Métiers ParisTech, 151 Boulevard de l'Hôpital, 75013 Paris, FRANCE

Abstract

Organic Rankine cycles are one of the available solutions for converting low grade heat source into electrical power. However the development of plants tends to be very expansive due to the specific design of the expander. Usually, the input parameters for designing an ORC plant are the temperature and power of the heat and cold sources. They lead to the selection of a working fluid, pressures and temperatures. The expander is then designed based on the required operating parameters. Using standard turbine easily available on the market and with well known performances would allow to reduce the development and manufacturing cost. However, the ORC would have to be adapted to make the expander work in its best conditions. For a solar concentrated heat source, the temperature and power can be adapted by adjusting the concentration factor and the collector total area. In this paper, a given gas turbine is considered to be used as the expander of the ORC. Knowing the turbine's performances with air, the optimal operating parameters (pressure, temperature, flow rate and rotational speed) of the ORC with different fluids are sought based on similitude rules. The adaptation aims to maintain same density evolution, same inlet speed triangle and same inlet Mach number with the working fluid as with air. The performance maps of the turbine are then computed with CFD simulations and showed a maximum isentropic efficiency close to the one with air, about 78%.

1. Introduction

Organic Rankine cycles are one of the available and efficient solutions to convert low grade heat source such as biomass, waste heat and solar into electrical power. However the development of plants tends to be expansive due to the design of specific parts, especially the vapor expanders. If big plants ($> 100kWe$) can afford the development cost of these specific parts, this is not the case for small scale ORC ($< 10kWe$). At this scale, the ORC technology would spread more quickly using standard components. Usually sizing the ORC system and expander is based on the hot and cold sources available temperatures and power.

Nomenclature

Δh Enthalpy drop [$J.kg^{-1}$]
P Pressure [Pa] or [bar]
T Temperature [K or [$°C$]
$\dot{m}$ Mass flowrate [$kg.s^{-1}$]
h Enthalpy [$J.kg^{-1}$]
U Blade speed [$m.s^{-1}$]
V Absolute speed [$m.s^{-1}$]
W Relative speed [$m.s^{-1}$]
a Sound speed [$m.s^{-1}$]
$\mathcal{M}$ Mach number
$\mathscr{P}$ Power [W]
C Torque [$N.m$]

Greek
α Absolute flow angle [°]
β Relative flow angle [°]
Γ Density ratio
η Efficiency
ρ Density [$kg.m^{-3}$]
ω Rotational speed [$rad.s^{-1}$]

Subscript
0   Turbine inlet
1   Impeller inlet
2   Turbine outlet
$fluid$ ORC working fluid
is Isentropic

When considering small scale ORC, the temperature and power might be adjusted as a compromise between the most efficient system and the affordable one. If considering a concentrated solar power (CSP) ORC, the hot source temperature and the available power can be easily adjusted by choosing the concentrating factor, temperature difference and the total surface of the collector.

In 2011, Quoilin [1] studied the adaptation of a standard scroll machine as an expander for the design of a low cost solar ORC to be installed in rural area of Lesotho. In 2014, Ferrara et al [2] analyzed the design options for a 20 kWe solar ORC. Depending of the hot source temperature, the solar ORC efficiency can be quite low (about 10%). It might be an interesting technology for combined heat and power, as the total efficiency will be increased with the use of residual heat. Freeman et al [3,4] demonstrated the potential of such a system for combined electric and heat production for a year round period in the UK. In all cases, thermal storage is required for stabilizing the ORC operation or to have continuous production [5].

In 2013, Wong et al [6] propose to design a 1 kWe ORC by selecting and converting a turbocharger. Recently While et al [7] adapted similitude theory for radial turbines using ORC working fluids. This will help improving the economy-of-scale [8] by having a given component (turbine or pump) able to work efficiently with different fluids.

In this paper, given an existing turbine, the operating parameters of an ORC are researched for an optimal operation of the turbine.

Rotational speed	230,000	rpm
Mass flow rate	0.046	kg/s
Adiabatic efficiency	0.78	-
Turbine inlet temperature T_0	873.15	K
Turbine inlet pressure P_0	3.21	bar
Outlet temperature T_2	680.15	K
Outlet pressure P_2	1.00	bar
Blade speed ratio	0.718	
Power output	8.92	kW

Table 1: Turbine design point characteristics

Inlet radius R_1	21.017	mm
Inlet tip b_1	2.538	mm
Relative inlet angle β_1	-40.675	°
Absolute inlet angle α_1	69.468	°
Outlet radius at hub R_{2h}	6.306	mm
Outlet radius at shroud R_{2s}	13.661	mm
Relative outlet angle at mid line β_{2m}	-50.471	°
Absolute outlet angle α_2	0.000	°
Relative outlet angle at hub β_{2h}	-35.685	°
Relative outlet angle at shroud β_{2s}	-57.273	°
Outlet tip b_2	7.356	mm
Number of blades Z	11	-

Table 2: Geometry parameters of turbine impeller

2. Original turbine operation

The geometry of the turbine is obtained by reverse engineering of an automotive turbocharger turbine. From the parameters at design point (Table 1), the geometry of the impeller is obtained using ANSYS turbo tools. The scroll housing is designed based on Stepanoff assumption (same velocity in each cross section).

The operating parameters at design point and the geometrical parameters of the standard turbine are presented in Table 1 and Table 2. The geometry of the turbine and the scroll housing are presented in Figures 1 and 2. The performance of the turbine fed with air are computed with the CFD model presented in section 4.1.
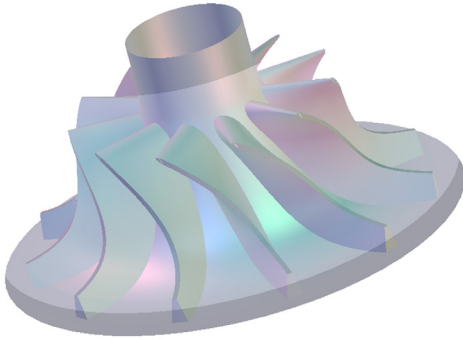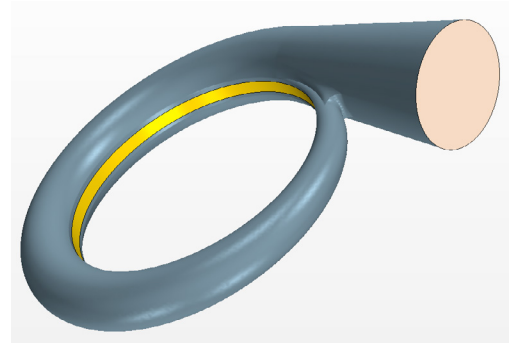

Fig. 1: Turbine wheel

Fig. 2: Scroll housing

3. Turbine operating point adaptation for working fluid

3.1. Assumption

Heat sink is the ambient air at temperature between 20 and 40°C. Heat source is a parabolic through fed with diathermic oil. Depending on the technology of the panel and the concentration factor, the oil temperature can range from 90°C to 250°C. A temperature difference of 5°C with the evaporating and condensing temperatures will be ensured in the heat exchangers as well as a subcooling of 5°C in the condenser. The temperatures difference may seem quite high and they would be easily reduced by improving the heat exchanger sizing. However this would add extra cost to the system.

The operating point of the turbine with the ORC working fluid is searched in order to ensure:

- Same inlet Mach number: $\mathcal{M}_1 = \frac{V_{1air}}{a_{0air}} = 0.870$

- Same density ratio: $\Gamma = \frac{\rho_{0\,air}}{\rho_{2\,air}} = 2.542$
- Same isentropic efficiency: $\eta_{is} = 0.78$

The efficiency of the thermodynamic cycle created with the turbine adaptation need to be evaluated. A simple ORC configuration is considered with only the solar heat collector, evaporator, condenser, pump and and turbine (see Figure 3). The power consumption of the oil circulating pump is negligible. The losses due to the cooling fan would depend on the amount of heat to dissipate and the temperature difference of the air flow. They have been neglected in this study. A proper estimation of theses would require the calculation of the air condensor parameters and might slightly change the results. The cycle efficiency is then expressed with eq. (1). This will allow for the determination of the operating point featuring the best thermal efficiency.

$$\eta_{cycle} = \frac{\mathscr{P}_{turbine\ fluid} - \mathscr{P}_{pump\ fluid}}{\mathscr{P}_{thermal\ fluid}} = \frac{\dot{m}_{fluid}(h_{0fluid} - h_{2fluid}) - \dot{m}_{fluid}/\rho_{0fluid}(P_{4fluid} - P_{3fluid})}{\dot{m}_{fluid}(h_{0fluid} - h_{4fluid})} \tag{1}$$
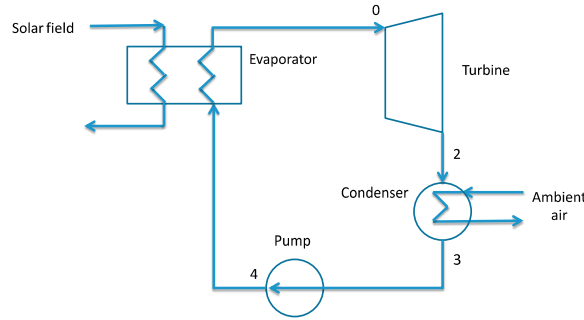

Fig. 3: Simple ORC configuration

3.2. Procedure

Starting with fixed inlet pressure P_{0fluid} and inlet temperature T_{0fluid}, the operating point of the turbine will be fully determined applying the following procedure:

1. Compute a_{0fluid}, ρ_{0fluid} and h_{0fluid} with CoolProp [9] from P_{0fluid} and T_{0fluid}
2. Compute $N_{fluid} = a_{0fluid}/a_{0air}\ N_{air}$
3. Compute $U_{1fluid} = R_1\ N_{fluid}\ \frac{\pi}{30}$
4. Compute $\Delta h_{is\ fluid} = -U_{1fluid}^2$
5. Compute $h_{2fluid} = h_{0fluid} + \Delta h_{is\ fluid}\ \eta_{is}$
6. Compute $\rho_{2fluid} = \rho_0/\Gamma$
7. Compute P_{2fluid}, T_{2fluid} with CoolProp from ρ_{2fluid} and h_{2fluid}
8. Compute $\dot{m}_{fluid} = \dot{m}_{air}\frac{\rho_{0fluid}}{\rho_{0air}}\frac{N_{fluid}}{N_{air}}$

As the evolution in the volute has not been modeled, the fluid entering the radial impeller is assumed to be tangent to the blades. In step 4, considering a radial turbine the inlet tangential velocity $V_{1\theta}$ is assumed equal to the peripheral velocity U_1. Thus the enthalpy drop is $\Delta h_{isfluid} = U_1 V_{\theta 1} = -U_{1fluid}^2$

3.3. Fluid selection

The operating point adaptation has been applied for different fluids. For each fluid the point providing the maximum thermal efficiency is stored. Figures 4 to 7 present the thermal efficiency versus the inlet temperature for different inlet pressure. For each fluid, for a given inlet pressure, the efficiency curves are limited on the left by the saturation temperature. It can be noticed, for example that for SES36 with an inlet pressure of 1 bar, the fluid evaporates at 36°C which is the limit of the curve and give an efficiency of 4.155%. On the right hand side, the graphs are limited by the maximum temperature of the fluid. For SES36 (Fig. 4) and R245fa (Fig. 5), an optimum set of inlet temperature and pressure can be found in the range between saturation temperature and maximum temperature. For R134a and R152a similar behavior can be noticed but the maximum thermal efficiency is located next to the maximum temperature at higher inlet pressure. Contrary to SES36 and R245fa, these two fluids have a wet saturation curve. For each fluid, the operating parameters for the point with the best thermal efficiency have been kept. Figure 8 to 11 present the influence of the inlet temperature on cycle efficiency, output power, rotational speed and condensation temperature. The best efficiency is given by R152a with 6.7% with an inlet temperature of 216.6°C. Siloxanes fluids give the lowest cycle efficiency.

R245fa and SES36 give respectively 4.9 and 4.3% with an inlet temperature of 110.7°C and 70.9°C. For both fluids, the condensation temperature is approximately 35°C. They produce respectively 3.0 kW at 58,645 rpm and 1.06 kW at 46,519 rpm. Theses two fluids are commonly used for low temperature ORC, so they will be retained for the rest of the study. The cycle realized in T-s diagram are presented in Figure 12 and Figure 13.
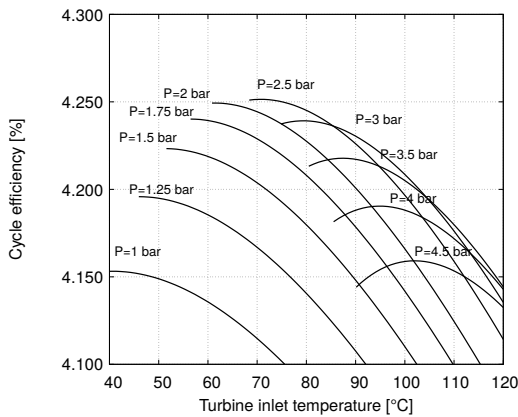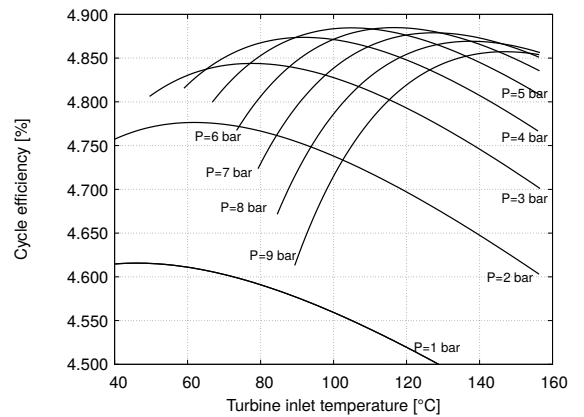

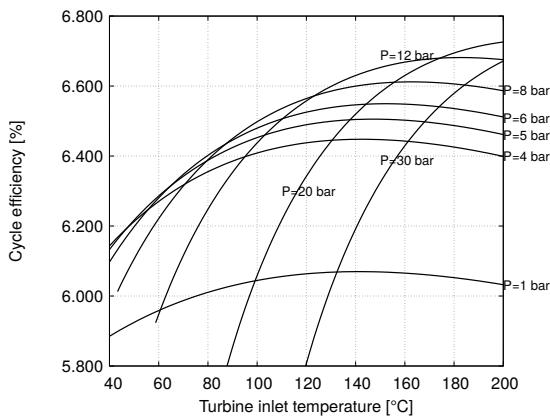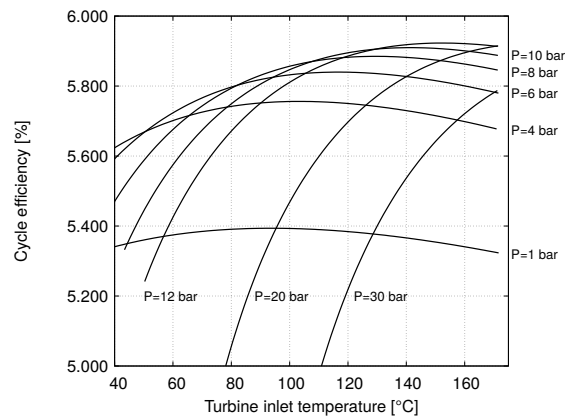
Fig. 4: SES36

Fig. 5: R245fa
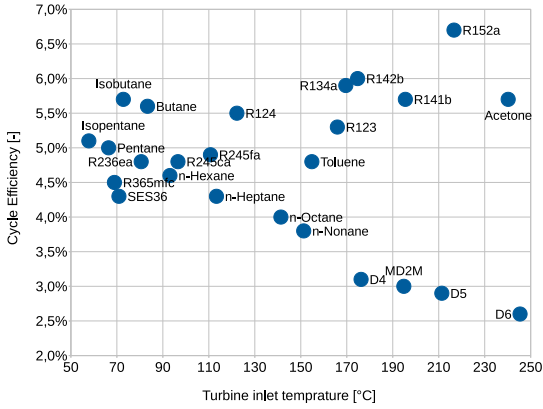

Fig. 6: R152a

Fig. 7: R134a
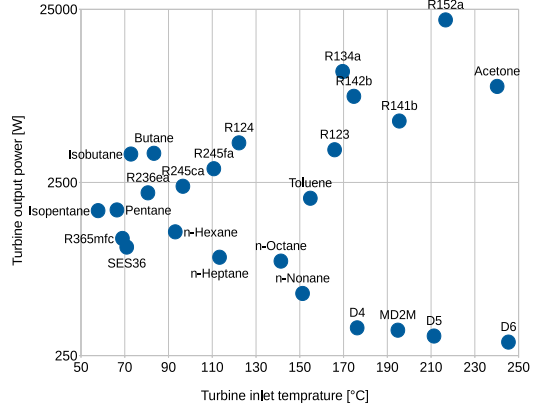
Fig. 8: Efficiency vs. inlet temperature

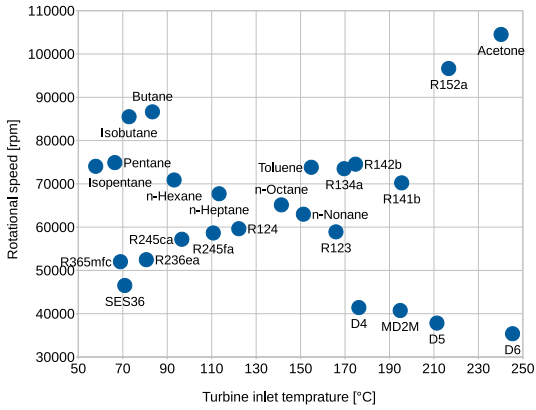Fig. 9: Turbine output power vs. inlet temperature

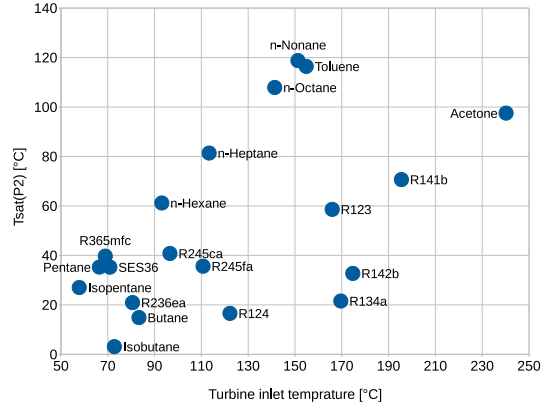Fig. 10: Rotational speed vs. inlet temperature

Fig. 11: Saturation temperature at turbine outlet pressure vs. inlet temperature
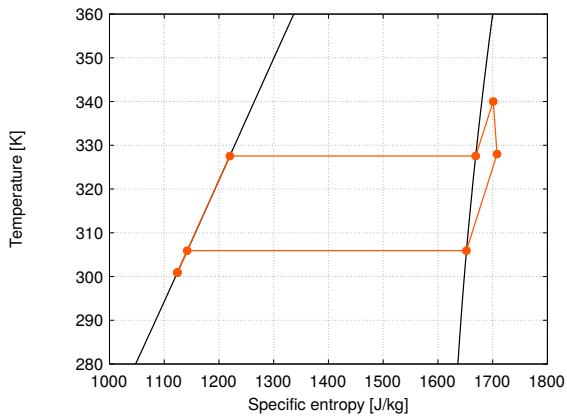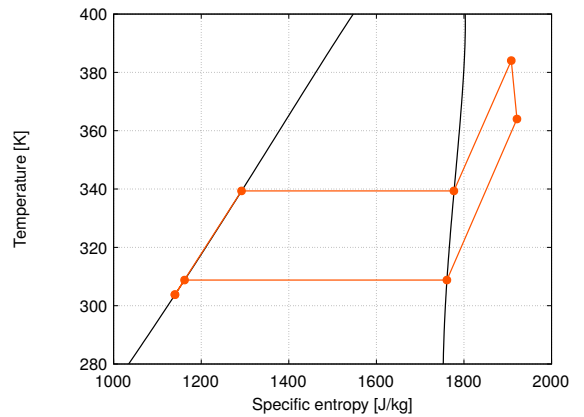

Fig. 12: T-s diagram - SES36

Fig. 13: T-s diagram - R245fa

4. CFD simulations

4.1. Model

The fluid volume of the model is extracted from the wheel presented Figure 1 and associated with the volume of the volute Figure 2. Frozen rotor simulations were carried out using StarCCM+. The mesh used the polyedral mesher with a base size of 2 mm and a prism layer of 2 cells. The total number of cells is 202,736.

A mesh sensitivity analysis has been carried out. On a finer mesh with 735,095 cells. The relative error on the results between the two different meshes is 0.04% on outlet temperature and 0.45% on inlet pressure and torque. Although the mesh is quite coarse, the same mesh will be used for all the simulations, so the results and tendency can be compared.

The simulations used the standard $k - \epsilon$ turbulence model. For the simulation with the air, the fluid is considered as an ideal gas. For the simulation with SES36 and R245fa, Peng-Robinson EOS is considered. The boundary conditions are mass flow inlet with a fixed temperature, pressure outlet and adiabatic walls.

The convergence is ensured by monitoring residuals decrease and asymptotic behavior of integral values such as inlet pressure, outlet temperature and outlet mass flow rate.

4.2. Results

For the turbine operating with air as an ideal gas, the isentropic efficiency can be easily determined with eq (2)

$$\eta_{turbine} = \frac{T_2 - T_0}{T_{2is} - T_0} \tag{2}$$

with $T_{2is} = T_0 \left(\frac{P_2}{P_0}\right)^{\left(\frac{\gamma-1}{\gamma}\right)}$

When operating with organic fluids the computation of the isentropic efficiency is replaced by eq (3). With $\Delta h_{is} = h_0 - h_{2is}$ and $h_{2is} = EoS(P_2, s_0)$ determined with CoolProp. C is the torque on the shaft.

$$\eta_{turbine} = \frac{\mathscr{P}_{shaft}}{\mathscr{P}_{is}} = \frac{C_{shaft}\,\omega}{\dot{m}\Delta h_{is}} \tag{3}$$

Figure 14 presents the turbine performance curve for original turbine fed with air. The maximum efficiency of the turbine with air at 230,000 rpm is 79.6%. It is a little higher than expected for the design point. The difference is mainly explained by the fact that the CFD model doesn't take into account the clearance between the wheel and the shroud.

Figure 15 presents the turbine performance curves for operations with SES36 and R245fa. For both graphs the mass flow rate has been corrected like for air: $\dot{m}_{corrected} = \dot{m}\sqrt{T_1/T_0}/(P_1/P_0)$ with $P_1 = 1\ bar$ and $T_1 = 293.15\ °C$. The turbine has an optimal operating point with an efficiency of 77.1% with SES36 and of 77.5% with R245fa. This is very close to the best efficiency obtained with air.
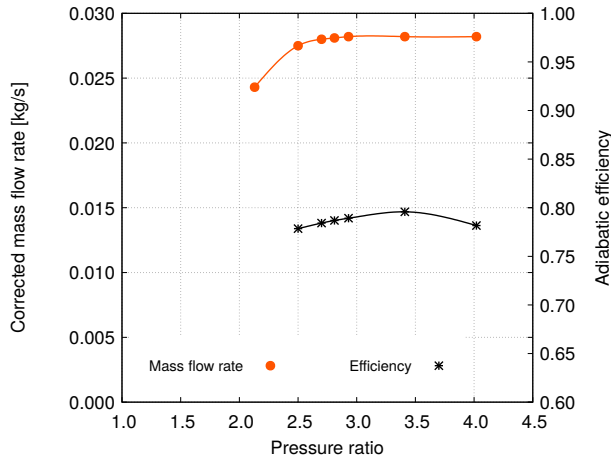
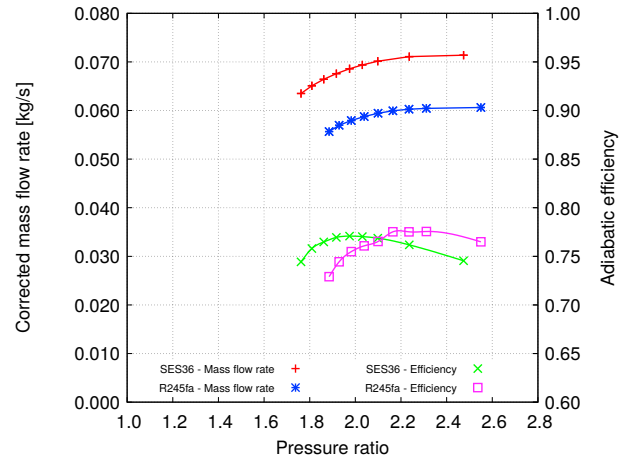Fig. 14: Original turbine performance with air
$N = 230,000 \, rpm$

Fig. 15: Adapted turbine performance with ORC fluid
$N_{SES36} = 46,519 \, rpm$ and $N_{R245fa} = 58,645 \, rpm$

Conclusion and perspectives

In this paper a given radial turbine has been studied for its potential to be used as a turbo expander of a solar ORC. A methodology based on simple similitude rules allow for the determination of the best operating while varying the inlet and outlet pressure for different fluids. CFD simulations of the turbine for two fluids confirmed the ability of the method to predict correctly the adapted best operating point.

Further developments will aim to adapt such a turbine and to test it on Arts et Métiers ParisTech ORC test bench. This will allow to compare CFD and experimental results and to study the off design behavior.

References

[1] S. Quoilin, M. Orosz, H. Hemond, V. Lemort, Performance and design optimization of a low-cost solar organic Rankine cycle for remote power generation, Solar Energy 85 (5) (2011) 955–966.

[2] F. Ferrara, A. Gimelli, A. Luongo, Small-scale concentrated solar power (CSP) plant: ORCs comparison for different organic fluids, Energy Procedia 45 (2014) 217–226.

[3] J. Freeman, K. Hellgardt, C. N. Markides, An assessment of solar-powered organic Rankine cycle systems for combined heating and power in UK domestic applications, Applied Energy 138 (2015) 605–620.

[4] J. Freeman, K. Hellgardt, C. N. Markides, Working fluid selection and electrical performance optimisation of a domestic solar-ORC combined heat and power system for year-round operation in the UK, Applied Energy 186 (2017) 291–303.

[5] E. Casati, A. Galli, P. Colonna, Thermal energy storage for solar-powered organic Rankine cycle engines, Solar Energy 96 (2013) 205–219.

[6] C. S. Wong, D. Meyer, S. Krumdieck, Selection and Conversion of Turbocharger As Turbo-Expander for Organic Rankine Cycle (Orc), 35th New Zealand Geothermal Workshop (November) (2013) 1–8.

[7] M. White, A. I. Sayma, The application of similitude theory for the performance prediction of radial turbines within small-scale low-temperature organic Rankine cycles, Journal of Engineering for Gas Turbines and Power 137 (12) (2015) 10.

[8] M. White, A. I. Sayma, Improving the economy-of-scale of small organic rankine cycle systems through appropriate working fluid selection, Applied Energy 183 (2016) 1227–1239.

[9] I. H. Bell, J. Wronski, S. Quoilin, V. Lemort, Pure and Pseudo-pure Fluid Thermophysical Property Evaluation and the Open-Source Thermophysical Property Library CoolProp, Industrial & Engineering Chemistry Research 53 (6) (2014) 2498–2508.